




# SARS-CoV-2-specific CD8<sup>+</sup> T-cell responses and TCR signatures in the context of a prominent HLA-A\*24:02 allomorph

Louise C Rowntree<sup>1</sup>, Jan Petersen<sup>2,3</sup> , Jennifer A Juno<sup>1</sup> , Priyanka Chaurasia<sup>2</sup>, Kathleen Wragg<sup>1</sup>, Marios Koutsakos<sup>1</sup>, Luca Hensen<sup>1</sup>, Adam K Wheatley<sup>1,4</sup>, Stephen J Kent<sup>1,4,5</sup>, Jamie Rossjohn<sup>2,3,6</sup>, Katherine Kedzierska<sup>1a</sup>  & Thi HO Nguyen<sup>1a</sup>

1 Department of Microbiology and Immunology, University of Melbourne at the Peter Doherty Institute for Infection and Immunity, Melbourne, VIC 3000, Australia

2 Infection and Immunity Program and Department of Biochemistry and Molecular Biology, Biomedicine Discovery Institute, Monash University, Clayton, VIC 3800, Australia

3 Australian Research Council Centre of Excellence for Advanced Molecular Imaging, Monash University, Clayton, VIC 3800, Australia

4 ARC Centre of Excellence in Convergent Bio-Nano Science and Technology, University of Melbourne, Melbourne, VIC 3000, Australia

5 Melbourne Sexual Health Centre, Infectious Diseases Department, Alfred Health, Central Clinical School, Monash University, Melbourne, VIC 3004, Australia

6 Institute of Infection and Immunity, Cardiff University School of Medicine, Heath Park, Cardiff, CF14 4XN, UK

## Keywords

CD8<sup>+</sup> T cells, COVID-19, HLA-A\*24:02, SARS-CoV-2 epitopes, T-cell receptor

## Correspondence

Katherine Kedzierska and Thi HO Nguyen, Department of Microbiology and Immunology, University of Melbourne at the Peter Doherty Institute for Infection and Immunity, Melbourne, VIC 3000, Australia. E-mails: kkedz@unimelb.edu.au (KK); thonguyen@unimelb.edu.au (TN)

<sup>a</sup>Authors contributed equally to this study.

Received 14 April 2021;

Revised 31 May 2021;

Accepted 2 June 2021

doi: 10.1111/imcb.12482

*Immunology & Cell Biology* 2021; **99**: 990–1000

## Abstract

In-depth understanding of human T-cell-mediated immunity in coronavirus disease 2019 (COVID-19) is needed if we are to optimize vaccine strategies and immunotherapies. Identification of severe acute respiratory syndrome coronavirus 2 (SARS-CoV-2) T-cell epitopes and generation of peptide–human leukocyte antigen (peptide–HLA) tetramers facilitate direct *ex vivo* analyses of SARS-CoV-2-specific T cells and their T-cell receptor (TCR) repertoires. We utilized a combination of peptide prediction and *in vitro* peptide stimulation to validate novel SARS-CoV-2 epitopes restricted by HLA-A\*24:02, one of the most prominent HLA class I alleles, especially in Indigenous and Asian populations. Of the peptides screened, three spike-derived peptides generated CD8<sup>+</sup>IFN $\gamma$ <sup>+</sup> responses above background, S<sub>1208–1216</sub> (QYIKWPWYI), S<sub>448–456</sub> (NINYLYRLF) and S<sub>193–201</sub> (VFKNIDGYF), with S<sub>1208</sub> generating immunodominant CD8<sup>+</sup>IFN $\gamma$ <sup>+</sup> responses. Using peptide–HLA-I tetramers, we performed direct *ex vivo* tetramer enrichment for HLA-A\*24:02-restricted CD8<sup>+</sup> T cells in COVID-19 patients and prepandemic controls. The precursor frequencies for HLA-A\*24:02-restricted epitopes were within the range previously observed for other SARS-CoV-2 epitopes for both COVID-19 patients and prepandemic individuals. Naïve A24/SARS-CoV-2-specific CD8<sup>+</sup> T cells increased nearly 7.5-fold above the average precursor frequency during COVID-19, gaining effector and memory phenotypes. *Ex vivo* single-cell analyses of TCR $\alpha\beta$  repertoires found that the A24/S<sub>448</sub><sup>+</sup>CD8<sup>+</sup> T-cell TCR $\alpha\beta$  repertoire was driven by a common TCR $\beta$  chain motif, whereas the A24/S<sub>1208</sub><sup>+</sup>CD8<sup>+</sup> TCR $\alpha\beta$  repertoire was diverse across COVID-19 patients. Our study provides an in depth characterization and important insights into SARS-CoV-2-specific CD8<sup>+</sup> T-cell responses associated with a prominent HLA-A\*24:02 allomorph. This contributes to our knowledge on adaptive immune responses during primary COVID-19 and could be exploited in vaccine or immunotherapeutic approaches.

## INTRODUCTION

The coronavirus disease 2019 (COVID-19) pandemic caused by the severe acute respiratory syndrome coronavirus 2 (SARS-CoV-2) has, as of June 2021, infected more than 170 million people, caused at least 3.5 million deaths<sup>1</sup> and paralyzed economies globally. International research efforts have led to the development of successful COVID-19 vaccine candidates, which have proven to be safe and effective in phase 2/3 clinical trials, especially against severe hospitalization and fatal disease outcomes.<sup>2,3</sup> While rolling out the vaccination programs globally, it is still important to develop an in-depth understanding on immune responses to SARS-CoV-2 infection so that immunopathology can be managed, immunotherapies optimized and universal next-generation vaccines designed rationally.

CD8<sup>+</sup> T cells play an important part in antiviral immunity by killing virally infected cells, producing antiviral cytokines such as interferon gamma (IFN $\gamma$ ), tumor necrosis factor (TNF) and interleukin-2 and establishing long-term and generally broadly cross-reactive immunological memory. Previous studies demonstrated that CD8<sup>+</sup> T cells become activated prior to recovery from COVID-19,<sup>4,5</sup> and survive into convalescence,<sup>6,7</sup> indicating an involvement of CD8<sup>+</sup> T cells in SARS-CoV-2 clearance and recovery. Both *in vitro* peptide stimulation assays and peptide-major histocompatibility complex-I tetramer approaches provided further evidence on activation, IFN $\gamma$  production and clonal proliferation of SARS-CoV-2-specific CD8<sup>+</sup> T cells.<sup>8–10</sup> Activated CD69<sup>+</sup>CD137<sup>+</sup>CD8<sup>+</sup> T cells directed toward overlapping megapeptide pools derived from spike (S), membrane (M), nucleocapsid (N) and ORF proteins could be detected in nearly 70% of acute and convalescent COVID-19 patients. Cross-reactive CD8<sup>+</sup> T-cell responses toward peptides derived from circulating human coronaviruses (hCoVs) have also been proposed in some individuals.<sup>11,12</sup>

To provide a better understanding of SARS-CoV-2-specific CD8<sup>+</sup> T cells in acute COVID-19, their persistence into long-term memory and subsequent recall following vaccination and/or infection, specific CD8<sup>+</sup> T-cell epitopes need to be identified. Several SARS-CoV-2 CD8<sup>+</sup> T-cell epitopes have recently been defined for human leukocyte antigen (HLA) class I alleles such as HLA-A\*01:01, A\*02:01, A\*03:01, A\*11:01, HLA-B\*07:02, B\*27:05, B\*40:01 and B\*44:03.<sup>8,11,13,14</sup> Identification of these SARS-CoV-2 CD8<sup>+</sup> T-cell specificities allowed us to determine the precursor frequency of SARS-CoV-2 tetramer-specific CD8<sup>+</sup> T cells in pre-pandemic samples,

acute COVID-19 and convalescence.<sup>8,9</sup> *Ex vivo* phenotypic analysis revealed that immunodominant B7/N<sub>105</sub><sup>+</sup>CD8<sup>+</sup> T-cell responses originated from high-frequency naïve pools found across HLA-B\*07:02-expressing individuals.<sup>9</sup> By contrast, A2/S<sub>269</sub><sup>+</sup>CD8<sup>+</sup> T cells were of suboptimal frequency and phenotypes.<sup>8</sup> The question remains whether SARS-CoV-2-specific CD8<sup>+</sup> T-cell responses generally reflect the immunodominant B7/N<sub>105</sub><sup>+</sup>CD8<sup>+</sup> or subdominant A2/S<sub>269</sub><sup>+</sup>CD8<sup>+</sup> T-cell responses. To answer this question, a broad range of SARS-CoV-2 CD8<sup>+</sup> T-cell specificities restricted across several dominant HLAs need to be identified and analyzed directly *ex vivo*.

In our study, we utilized a combination of peptide prediction and *in vitro* peptide stimulation to identify novel SARS-CoV-2 epitopes restricted by one of the most frequent HLA class I, especially in Indigenous and Asian populations, HLA-A\*24:02. Of the peptides screened, three spike-derived peptides generated CD8<sup>+</sup>IFN $\gamma$ <sup>+</sup> responses above background, S<sub>1208–1216</sub> (QYIKWPWYI), S<sub>448–456</sub> (NYNYLYRLF) and S<sub>193–201</sub> (VFKNIDGYF), with S<sub>1208</sub> generating the strongest CD8<sup>+</sup>IFN $\gamma$ <sup>+</sup> responses. Using peptide–HLA-I tetramers, we performed direct *ex vivo* tetramer enrichment for A24/S<sub>1208</sub><sup>+</sup>CD8<sup>+</sup> and A24/S<sub>448</sub><sup>+</sup>CD8<sup>+</sup> T cells in HLA-A\*24:02-expressing COVID-19 patients and pre-pandemic controls. We found that CD8<sup>+</sup> T cells directed at both HLA-A\*24:02-restricted epitopes had similar frequencies and activation phenotypes in COVID-19 patients, whereas the frequencies in pre-pandemic samples were comparable to those of A2/S<sub>269</sub><sup>+</sup>CD8<sup>+</sup> T cells.<sup>8</sup> A24/S<sub>448</sub><sup>+</sup>CD8<sup>+</sup> T-cell and A24/S<sub>1208</sub><sup>+</sup>CD8<sup>+</sup> T-cell responses had contrasting T-cell receptor  $\alpha\beta$  (TCR $\alpha\beta$ ) repertoires, where the A24/S<sub>448</sub><sup>+</sup>CD8<sup>+</sup> TCR $\alpha\beta$  repertoire was driven by a common TCR $\beta$  chain motif, whereas the A24/S<sub>1208</sub><sup>+</sup>CD8<sup>+</sup> TCR $\alpha\beta$  repertoire was diverse across COVID-19 patients.

## RESULTS

### CD8<sup>+</sup> T cells respond to HLA-A\*24:02-restricted SARS-CoV-2 epitopes

In this study, we recruited eight HLA-A\*24:02-expressing individuals: four HLA-A\*24:02<sup>+</sup> convalescent COVID-19 patients from community infections (median age 63 years, range 52–75, 100% male, range 71–217 days post-symptom onset) and four HLA-A\*24:02<sup>+</sup> pre-pandemic healthy controls (median age 36 years, range 24–59, 100% male).

Using the COVID-19 donors, we probed for SARS-CoV-2-specific CD8<sup>+</sup> T cells recognizing predicted HLA-

A\*24:02-binding peptides from the SARS-CoV-2 S, N and M proteins based on the NetCTLpan prediction algorithm (Figure 1a; accessed May 2020). Peripheral blood mononuclear cells from four convalescent HLA-A\*24:02<sup>+</sup> COVID-19 patients were expanded *in vitro* with a pool of either 12 S (pool 1) or 10 M or N (pool 2) predicted A24/SARS-CoV-2 peptides for 12 days, then restimulated with individual peptides in an intracellular cytokine staining assay to determine peptide immunogenicity (Figure 1b). Of the 12 S peptides screened, three peptides generated CD8<sup>+</sup>IFN $\gamma$ <sup>+</sup> responses above background (dimethyl sulfoxide control): S<sub>1208–1218</sub> (QYIKWPWYI), S<sub>448–456</sub> (NYYLYRLF) and S<sub>193–201</sub> (VFKNIDGYF) (Figure 1c). S<sub>1208</sub> generated the strongest CD8<sup>+</sup>IFN $\gamma$ <sup>+</sup> response in three of four donors tested (mean 9.73%), with S<sub>448</sub> and S<sub>193</sub> responses observed in two (mean 3.85%) and one (3.37%) donors, respectively (Figure 1d). Only one donor showed responses to the M and N pool, with very small IFN $\gamma$  production (~1%) to four of the six M peptides tested that was not able to be narrowed to a single epitope.

Peptide sequence conservation analysis for the S-derived SARS-CoV-2 immunogenic peptides was extended to previously circulating coronaviruses. SARS-CoV-2 S<sub>1208</sub>, S<sub>448</sub> and S<sub>193</sub> peptide sequences were compared with reference protein sequences for the hCoV strains NL63, 229E, HKU1 and OC43 (Figure 2a). The SARS-CoV-2/S<sub>1208</sub> epitope shared 66% sequence identity with all of the hCoV strains. All hCoV strains displayed differences at position 1 and 9 (anchor residue), in addition to variation at either position 3 (HKU1 and OC43) or 8 (NL63 and 229E). Sequence conservation was lower for S<sub>448</sub> and S<sub>193</sub> peptides, where sequence identity ranged between 44% and 55%. More of these amino acid variations occurred at position 2 (anchor residue) and we therefore predict that analogous hCoV peptides are unlikely to be HLA-A\*24:02 ligands, though this is yet to be formally determined.

#### A24/SARS-CoV-2-specific CD8<sup>+</sup> T cells are increased in COVID-19 patients compared with prepandemic donors

To further analyze the SARS-CoV-2-specific A24/CD8<sup>+</sup> populations, tetramer-associated magnetic enrichment<sup>15,16</sup> was performed to determine the *ex vivo* frequencies of A24/S<sub>1208</sub><sup>+</sup>CD8<sup>+</sup> and A24/S<sub>448</sub><sup>+</sup>CD8<sup>+</sup> T cells in HLA-A\*24:02<sup>+</sup> COVID-19 patients and prepandemic controls (Figure 2b). The precursor frequency of A24/S<sub>448</sub><sup>+</sup>CD8<sup>+</sup> T cells in COVID-19 convalescent donors (mean  $6.3 \times 10^{-5}$ ,  $n = 4$ ) was significantly higher than that observed in prepandemic healthy individuals (mean  $8.44 \times 10^{-6}$ ,  $n = 4$ ,

$P = 0.0286$ ) (Figure 2c, left panel). The precursor frequencies of A24/S<sub>448</sub><sup>+</sup>CD8<sup>+</sup> T cells were comparable to the previously observed frequencies of A24/S<sub>1208</sub><sup>+</sup>CD8<sup>+</sup> T cells (mean  $7.71 \times 10^{-5}$  for COVID-19 convalescents and  $9.50 \times 10^{-6}$  for prepandemic donors<sup>9</sup>), with most donors having similar frequencies of both epitopes (Figure 2c, right panel). Furthermore, the precursor frequencies for both SARS-CoV-2 HLA-A24 epitopes were within the range previously observed for other SARS-CoV-2 epitopes for both COVID-19 patients and prepandemic individuals.<sup>8,9</sup> Finally, the percentage of both the A24/S<sub>448</sub><sup>+</sup>CD8<sup>+</sup> and A24/S<sub>1208</sub><sup>+</sup>CD8<sup>+</sup> T cells increased, though not significantly, after 12 days of stimulation with the S peptide pool in 2 and 3 COVID-19 donors, respectively (Figure 2d). Evidently, the SARS-CoV-2-specific CD8<sup>+</sup> T cells were primed by SARS-CoV-2 in the COVID-19 individuals and are thus, at least under *in vitro* conditions, capable of clonal expansion. Overall, our data suggest that naïve A24/SARS-CoV-2-specific CD8<sup>+</sup> T cells can be expanded nearly 7.5-fold following COVID-19.

#### Different activation profiles of SARS-CoV-2-specific A24/S<sub>448</sub><sup>+</sup>CD8<sup>+</sup> T cells in COVID-19 and healthy individuals

The activation profiles of A24/S<sub>448</sub><sup>+</sup>CD8<sup>+</sup> T cells tested directly *ex vivo* from COVID-19 patients and prepandemic healthy individuals were assessed by CD27, CD45RA and CD95 staining to determine the prevalence of the naïve (CD27<sup>+</sup>CD45RA<sup>+</sup>CD95<sup>-</sup>), stem cell memory (CD27<sup>+</sup>CD45RA<sup>+</sup>CD95<sup>+</sup>), central memory-like (CD27<sup>+</sup>CD45RA<sup>-</sup>), effector memory-like (CD27<sup>-</sup>CD45RA<sup>-</sup>) and effector memory CD45RA (CD27<sup>-</sup>CD45RA<sup>+</sup>) T-cell subsets (Figure 2b). The phenotype of the A24/S<sub>448</sub><sup>+</sup>CD8<sup>+</sup> T cells was highly varied across the convalescent COVID-19 donors, with the majority of the tetramer-positive CD8<sup>+</sup> T cells being stem cell memory ( $n = 2$ ), effector memory CD45RA ( $n = 1$ ) or naïve ( $n = 1$ ) (Figure 2e). Conversely, the prevalence of the naïve phenotype (mean of 73%) was significantly enriched in prepandemic individuals compared with convalescent COVID-19 patients ( $P = 0.0008$ ). This phenotypic pattern in both the COVID-19 patients and prepandemic healthy individuals aligns with what has been previously observed for other SARS-CoV-2-specific CD8<sup>+</sup> T cells, including A24/S<sub>1208</sub><sup>+</sup>CD8<sup>+</sup> T cells.<sup>9</sup> The prepandemic individuals displayed a mainly naïve profile (mean of 61%), whereas the A24/S<sub>1208</sub>-specific CD8<sup>+</sup> T cells in the COVID-19 donors were more skewed toward naïve ( $n = 2$ ), central memory ( $n = 1$ ) or effector memory CD45RA ( $n = 1$ ) T-cell phenotypes.<sup>9</sup>

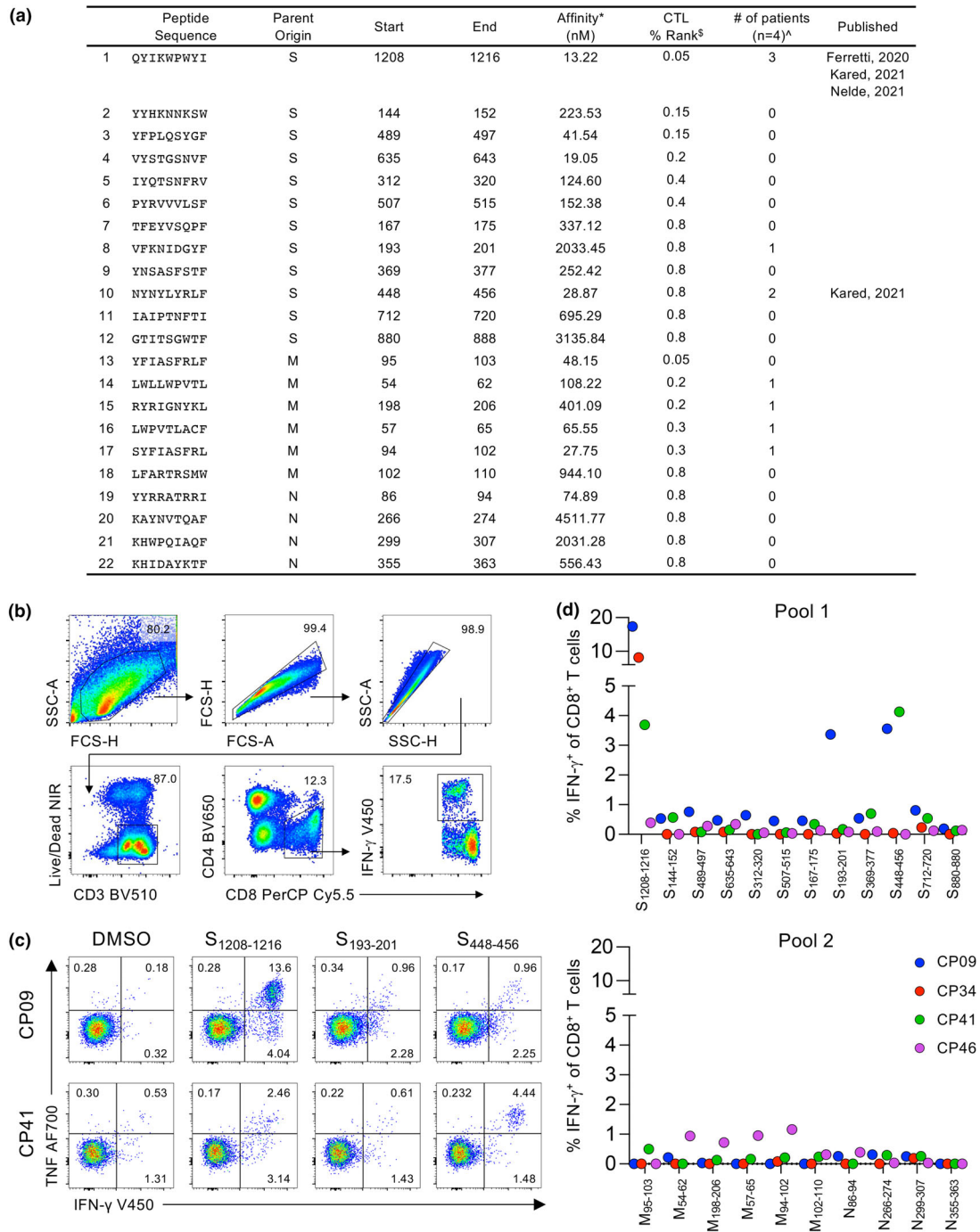


**Figure 1.** Identification of SARS-CoV-2-specific HLA-A\*24:02-restricted CD8<sup>+</sup> T-cell epitopes. **(a)** List of peptides predicted to bind HLA-A\*24:02. \*Affinity (equilibrium dissociation constant) predicted using NetMHCpan. <sup>§</sup>CTL percentage rank predicted using NetCTLpan. <sup>^</sup>Number of COVID-19 donors functionally responding by ICS in this study. See also Kared *et al.*<sup>10</sup>, Ferretti *et al.*<sup>11</sup> and Nelde *et al.*<sup>23</sup> **(b)** Gating strategy of IFN $\gamma$ -producing CD8<sup>+</sup> T cells following ICS. **(c)** Representative flow cytometry plots of CD8<sup>+</sup> IFN $\gamma$ /TNF staining after stimulation with the SARS-CoV-2 peptides S<sub>1208-1216</sub>, S<sub>193-201</sub> and S<sub>448-456</sub> presented by C1R.A\*24:02 cells. **(d)** Frequencies of IFN $\gamma$ <sup>+</sup> of CD8<sup>+</sup> T cells for each SARS-CoV-2 peptide, with background (DMSO) staining subtracted (*n* = 4). Peptide screen was performed in convalescent COVID-19 PBMCs after 12-day expansion *in vitro* with pooled S (pool 1) or M and N peptides (pool 2). CTL, cytotoxic T lymphocyte; COVID-19, coronavirus disease 2019; DMSO, dimethyl sulfoxide; FCS-A, forward scatter–area; FCS-H, forward scatter–height; HLA, human leukocyte antigen; ICS, intracellular cytokine staining; IFN, interferon; PBMCs, peripheral blood mononuclear cells; SARS-CoV-2, severe acute respiratory syndrome coronavirus 2; SSC-A, side scatter–area; SSC-H, side scatter–height; TNF, tumor necrosis factor.

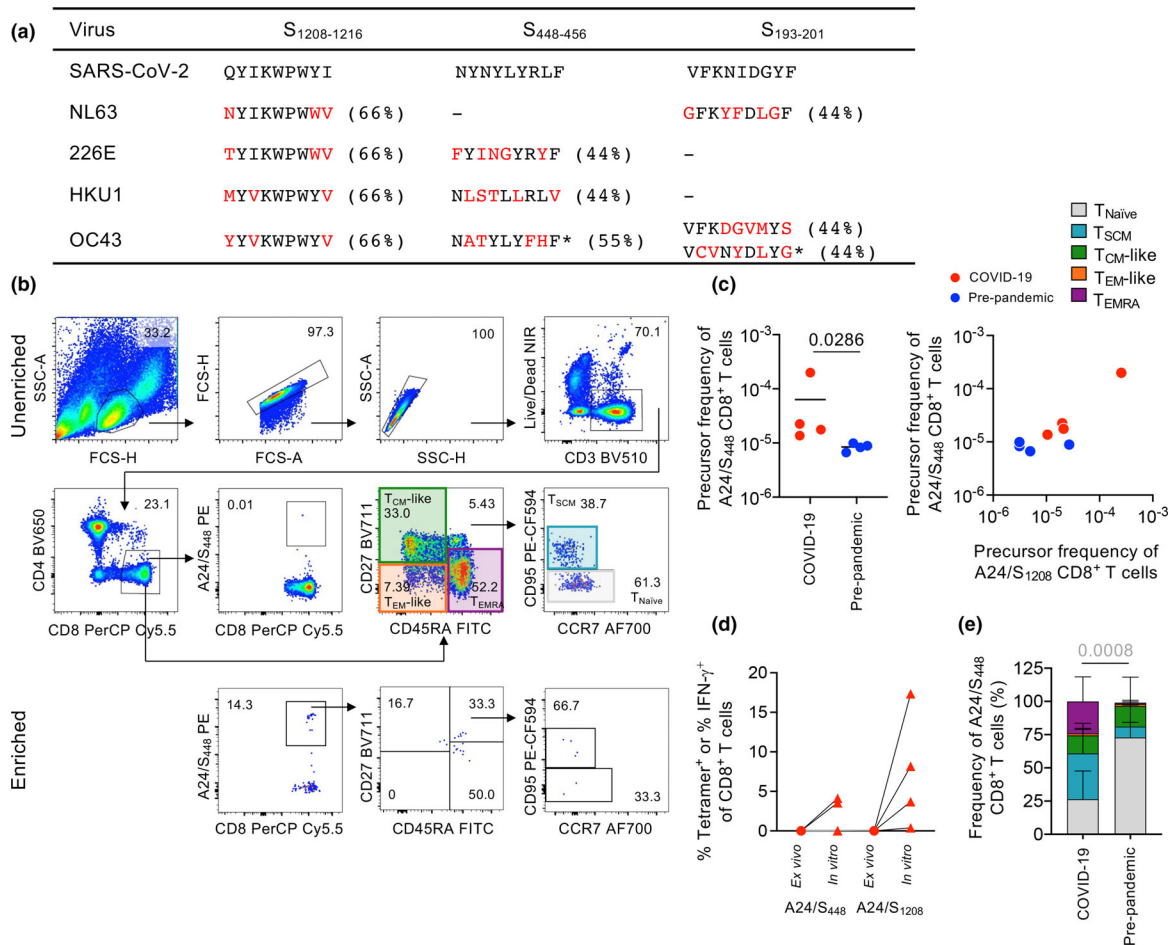


**Figure 2.** Phenotypes of SARS-CoV-2-specific A24/CD8<sup>+</sup> T cells. **(a)** List of SARS-CoV-2 peptide sequences and their homology with hCoV. Variable amino acids shown in red; \*unlikely to be HLA-A\*24:02 ligand; – no significant homology. **(b)** Gating strategy for phenotype analysis of tetramer<sup>+</sup> CD8<sup>+</sup> T cells in the unenriched fraction (top panels), which was used to gate enriched tetramer<sup>+</sup> CD8<sup>+</sup> T cells (bottom panels). **(c)** Precursor frequency of A24/S<sub>448-456</sub> CD8<sup>+</sup> T cells (of CD8<sup>+</sup> T cells) between COVID-19 and prepandemic individuals (left panel) and against A24/S<sub>1208-1216</sub> CD8<sup>+</sup> T-cell frequencies (right panel). **(d)** Frequencies of A24/SARS-CoV-2<sup>+</sup>CD8<sup>+</sup> T cells in the CD8<sup>+</sup> population in convalescent COVID-19 donors on day 0 and day 12 of expansion. *Ex vivo* frequency measured by tetramer<sup>+</sup> staining and *in vitro* frequency determined by IFN $\gamma$ <sup>+</sup> staining. **(e)** Stacked graphs of each phenotype subset within A24/S<sub>448-456</sub> CD8<sup>+</sup> T cells (of CD8<sup>+</sup> T cells) between COVID-19 and prepandemic individuals (mean with SD is shown). Exact *P*-values are shown where statistical significance was determined with the two-tailed **(c)** Mann–Whitney *U*-test and **(e)** Šidák’s multiple comparisons test. COVID-19, coronavirus disease 2019; FCS-A, forward scatter–area; FCS-H, forward scatter–height; FITC, fluorescein isothiocyanate; HLA, human leukocyte antigen; IFN, interferon; SSC-A, side scatter–area; SSC-H, side scatter–height; PE, phycoerythrin; SARS-CoV-2, severe acute respiratory syndrome coronavirus 2; T<sub>CM</sub>, central memory T cells; T<sub>EM</sub>, effector memory T cells; T<sub>EMRA</sub>, effector memory CD45RA T cell; T<sub>SCM</sub>, stem cell memory T cells.

### A24/S<sub>448</sub><sup>+</sup>CD8<sup>+</sup> TCR $\alpha\beta$ repertoire is driven by a common TCR $\beta$ chain

CD8<sup>+</sup> T-cell immunodominance, functionality and protection are all impacted by the molecular signature of the TCR repertoire.<sup>17-19</sup> Thus, using direct *ex vivo* tetramer staining and human single-cell TCR $\alpha\beta$  multiplex reverse transcription-PCR,<sup>15,20</sup> we determined the TCR $\alpha\beta$  clonal composition and diversity. We dissected the TCR $\alpha\beta$  repertoires for A24/S<sub>448</sub> and A24/S<sub>1208</sub>-specific

CD8<sup>+</sup> T cells in peripheral blood mononuclear cells from four HLA-A\*24:02-expressing COVID-19 patients, examining the TCR sequence for a total of 48 SARS-CoV-2-specific CD8<sup>+</sup> T cells (Figure 3a; Table 1).

The overall diversity of the TCR $\alpha\beta$  sequences was analyzed, first focusing on the TRBV region (Figure 3b). For A24/S<sub>448</sub><sup>+</sup>CD8<sup>+</sup> T cells, all donors had TRBV2 gene usage where one key TCR $\beta$  motif within the CDR3 $\beta$  loop was found across the COVID-19 patients, despite the fact that a limited number of A24/S<sub>448</sub>-specific sequences were

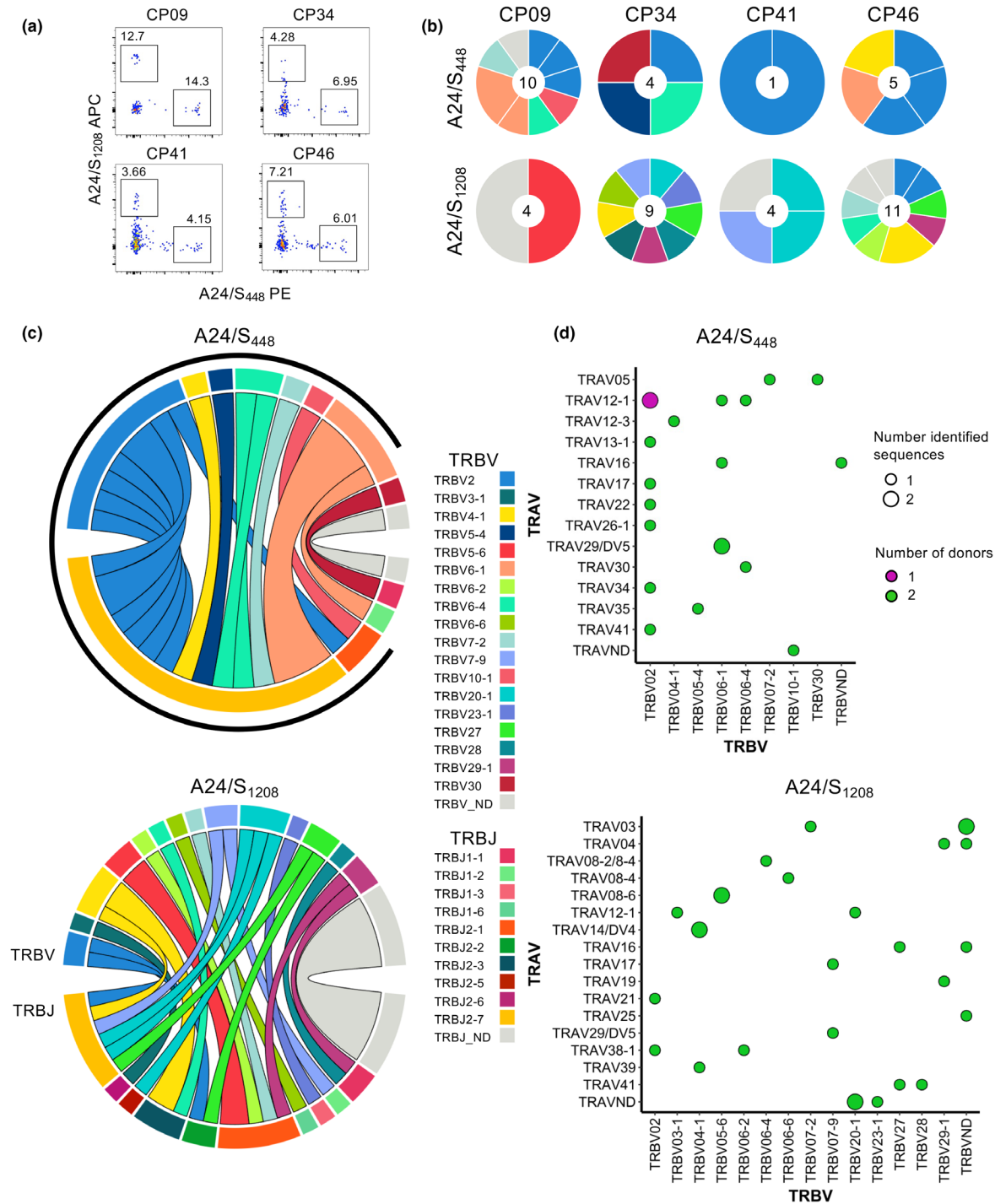


**Figure 3.** SARS-CoV-2-specific A24/CD8<sup>+</sup> T cells have different TCRαβ repertoire diversity. **(a)** FACS profiles of enriched A24/S<sub>448-456</sub><sup>+</sup> and A24/S<sub>1208-1216</sub><sup>+</sup> CD8<sup>+</sup> T cells from four COVID-19 donors, which were single-cell index sorted for TCRαβ analysis. **(b)** Pie charts of TRBV gene usage. Segments shown by the same color represent TCRβ clonotypes with the same TRBV segment usage but different TRBJ segments or CDR3 sequences. **(c)** Circos plots of TRBV and TRBJ segment linking; top arch and segment color indicate TRBV usage and bottom outer arch color depicts TRBJ usage. Surrounding black arc depicts the common CDR3β motif for A24/S<sub>448</sub><sup>+</sup> CD8<sup>+</sup> T cells. **(d)** Bubble plot showing the distribution (number of donors and sequences) of TRBV/TRAV gene usage in COVID-19 patients. APC, allophycocyanin; COVID-19, coronavirus disease 2019; FACS, fluorescence-activated cell sorting; PE, phycoerythrin; SARS-CoV-2, severe acute respiratory syndrome coronavirus; TCR, T-cell receptor.

**Table 1.** Full list of paired  $\alpha$  and  $\beta$  TCR gene usage and CDR3 amino acid sequence.

	TRBV	TRBJ	CDR3b	TRAV	TRAJ	CDR3a	09	34	41	46
A24/S <sub>448</sub>	2	2-7	CASSETGGYEQYF	22	13	CAPRD#NSGGYQKVTF	1			
	2	2-7	CASSESGQYEQYF	12-1	12	CVVVRMDSSYKLIF	1			
	2	2-1	CASSEGGQYEQFF	26-1	4	CIVYNKLIF	1			
	2	2-7	CASSEGGQYEQYF	13-1	15	CAARPEPTSTGTALIF				1
	2	2-7	CASASGQYEQYF	12-1	33	CVVNDLVDSNYQLW				1
	2	2-7	CASASGQYEQYF	41	33	ND				1
	2	2-7	CASSEFRSYEQYF	34	3	CGAA*R#ASKIIF		1		
	2	2-7	CASSRSGSVSYEQYF	17	4	CAXFFWW#YNKLIF			1	
	10-1	2-1	CASSEGGQYEQFF	ND	ND	ND	1			
	6-4	2-7	CASSEGGQYEQYF	12-1	28	ND	1			
	6-4	2-7	CASSETGGYEQYF	30	3	CGTES##YSSASKIIF		1		
	5-4	2-7	CASSLLGGYEQYF	35	42	CAGQ#GSGGNLIF		1		
	6-1	2-7	CASSETGGYEQYF	12-1	53	CVVNMLYSGGSNYKLTF	1			
	6-1	2-7	CASSETGGYEQYF	29/DV5	27	CAARH##AGKSTF	2			
	7-2	2-7	CASSLASGYEQYF	5	17	CAESMMEAAGNKLTF	1			
	4-1	2-7	CASSQGGPYEQYF	12-3	39	XAFFNKAGNXLXF				1
	6-1	1-2	CASSEWGGVAYGYTF	16	52	FAPXAGXXXXGKXTF				1
	30	1-1	CAWSVTGVTEAFF	5	11	CAEMNSGYSTLTF		1		
	ND	ND	ND	16	54	CALKDPLMAVQGAQKLVF	1			
	A24/S <sub>1208</sub>	2	2-2	CAGKSTGELFF	21	27	CAVRHTNAGKSTF			
2		2-7	ND	38-1	49	CAFMKINQFYF				1
3-1		2-6	CASCPSWGSANVLT	12-1	9	CVPNTGGFKTIF		1		
4-1		2-7	CASSVGATGAYEQYF	39	33	ND		1		
4-1		2-3	CASSQDYWGGGADTQYF	14/DV4	39	CAMREGQGNAGNMLTF				2
5-6		2-1	CASSQSGGGEQFF	8-6	17	CAVSEVGNLTF	2			
6-2		2-1	CASSWNLGAGDEQFF	38-1	52	CAFLNAGGTSYGKLT				1
6-4		2-3	CASSALVAFSTDTQYF	8-2/8-4	23	CAVYNQGGKLI				1
6-6		1-6	CASSFHPGQDRGNSPLHF	8-4	5	CAVSEGR#GRRALTF		1		
7-2		2-1	CASSSLAGEVNEQFF	3	21	CAVRALYNFNKIFYF				1
7-9		2-7	CASSLVGEGRGREQYF	17	12	CATEARMDSYKLIF		1		
7-9		1-2	CASSLGETIYGTYF	29/DV5	29	CAARSNTPLVF				1
20-1		2-7	CSARDQDRAYEQYF	12-1	47	CVVIEGNKLVF		1		
20-1		2-5	CSALNLD#QETQYF	ND	ND	ND				1
20-1		2-7	CSARTISQGAHYEQYF	ND	ND	ND				1
23-1		1-3	CASSGTDS#SGNTIYF	ND	ND	ND		1		
27		2-7	CASSLSTTTASYEQYF	16	18	CALRARGSTLGRLYF		1		
27		2-2	CASSYTQRGLDYTGELFF	41	34	CAVESYNTDKLIF				1
28		1-1	CASPWGAEAFF	41	44	CAVDTGTASKLTF		1		
29-1		2-1	CSVDPGQFYNEQFF	19	3	CALSYSSASKIIF		1		
29-1		1-1	CSVEDPMGVGTEAFF	4	6	ND				1
ND		ND	ND	3	25	CAVRDIRGQGFISFIF	2			
ND		ND	ND	25	17	CAGQ#AAGNKLTF				1
ND		ND	ND	16	27	CALSGEGG#TNAGKSTF				1
ND		ND	ND	4	9	CLVGENSGGFKTIF				1
						Total	14	13	5	16

ND = not determined; X = unresolved amino acid; \* = stop codon; # = out-of-frame shift.

examined per donor (1–10 cells/donor; Table 1). This motif was dominated by the TRBV2/TRBJ2-7 CAS(S/A)XXXGYEQYF (where X denotes any amino) sequence found in all COVID-19 patients (40% of the total TCR repertoire). This same CDR3 $\beta$  loop motif was also identified when TRBJ2-7 or 2-1 linked with five different

TRBV segments, TRBV5-4, 6-1, 6-4, 7-2 and 10-1 found across two of the four COVID-19 patients (40% of the total TCR repertoire). Similar CDR3 $\beta$  loops were also identified in a third donor, composed of TRBV4-1/TRBJ2-7 gene segments. Overall, the sequences with this CDR3 $\beta$  loop comprised 85% of the A24/S<sub>448</sub>-specific

repertoire (Figure 3c). The CDR3 $\beta$  loop motif paired with a range of different TRAV/TRAJ gene segments (Figure 3d) and therefore A24/S<sub>448</sub><sup>+</sup>CD8<sup>+</sup> T-cell specificity was likely driven by the TCR $\beta$  chain rather than the TCR $\alpha$  chain.

By contrast, the A24/S<sub>1208</sub>-specific CD8<sup>+</sup> TCR $\alpha\beta$  repertoire (4–11 cells/donor) was generally diverse, with almost all sequences identified only once and no TCR $\alpha\beta$  clonotypes overlapping between individuals. Each donor had distinct usage of TRAV, TRBV and TRAJ gene segments, with no common motifs within CDR3 $\alpha$  and CDR3 $\beta$  sequences. Interestingly, the TRBJ2-7 and 2-1 were enriched in the A24/S<sub>1208</sub>-specific CD8<sup>+</sup> TCR $\alpha\beta$  repertoire, represented in 26% and 22% of the sequenced TCR $\beta$  chains, respectively (Figure 3c). Overall, the common motif suggests more rigid requirements for TCR $\alpha\beta$  clones recognizing the A24/S<sub>448</sub> epitope compared with the A24/S<sub>1208</sub> epitope. The lack of TCR $\alpha\beta$  plasticity may explain the low naïve precursor frequency observed for A24/S<sub>448</sub>, similar to what has been previously observed for A2/S<sub>269</sub><sup>8</sup>; however, more data may be needed to determine the driving factors for A24/S<sub>1208</sub> recognition.

## DISCUSSION

HLA-A\*24:02 is one of the most prominent class I HLA alleles worldwide, especially widely expressed in the Indigenous and Asian populations. In comparison its 10% global distribution, HLA-A\*24:02 is of the highest frequency in Oceania (37%), North-East Asia (32.9%), Australia (21.4%) and Central and South America (20.6%).<sup>21</sup> Specifically, HLA-A\*24:02 is highly expressed in Indigenous Taiwan Paiwan (96.1%), Papua New Guinea Karimui Plateau Pawaia (74.4%), New Caledonia (60.7%), Alaskan Yupik (58.1%), New Zealand Maori (38%), Chile Easter Island (35.8%), American Samoans (33%) and Australian Aboriginal people (24%),<sup>21</sup> demonstrating its prominence in Indigenous people. As Indigenous people are susceptible to severe respiratory diseases such as influenza and HLA-A\*24:02 was associated with influenza-induced mortality during the 2009-pH1N1 outbreak,<sup>22</sup> identification of SARS-CoV-2-specific CD8<sup>+</sup> T-cell epitopes restricted by HLA-A\*24:02 is essential to understand the relationship between HLA-A\*24:02 and disease susceptibility in future studies.

Using peptide prediction tools in combination with an *in vitro* peptide stimulation, we identified SARS-CoV-2 epitopes restricted by HLA-A\*24:02, namely, three spike-derived peptides, S<sub>1208–1216</sub> (QYIKWPWYI), S<sub>448–456</sub> (NYYLYRLF) and S<sub>193–201</sub> (VFNIDGYF), with S<sub>1208</sub> generating the strongest CD8<sup>+</sup>IFN $\gamma$ <sup>+</sup> responses. Both A24/

S<sub>1208–1216</sub> and A24/S<sub>448–456</sub> have been recently independently identified by other groups.<sup>10,11,23</sup> Although all three SARS-CoV-2-derived peptides shared 44–66% sequence identity with hCoVs, the variations occur in either the anchor residues or likely TCR contact residues, suggesting a potential to escape preexisting CD8<sup>+</sup> T-cell immunity and supported by our observation of predominantly naïve A24/S<sub>1208</sub>- and A24/S<sub>448</sub>-specific CD8<sup>+</sup> T cells in pre-pandemic individuals. Using peptide–HLA-I tetramers, we performed direct *ex vivo* tetramer enrichment for HLA-A\*24:02-restricted CD8<sup>+</sup> T cells in COVID-19 patients and pre-pandemic controls. The precursor frequencies for HLA-A\*24:02-restricted epitopes were within the range previously observed for other SARS-CoV-2 epitopes such as HLA-A\*02:01-restricted S<sub>269</sub> for both COVID-19 patients and pre-pandemic individuals.<sup>8</sup> Thus, it appears that 5–10-fold expansion of SARS-CoV-2-specific CD8<sup>+</sup> T-cell responses is prototypical for the primary COVID-19, with the exception of B7/N<sub>105</sub><sup>+</sup>CD8<sup>+</sup> T-cell responses.<sup>9</sup> Similarly, the phenotypic pattern of the A24/S<sub>448</sub><sup>+</sup> and A24/S<sub>1208</sub><sup>+</sup>CD8<sup>+</sup> T cells aligns with previous SARS-CoV-2 epitopes, with pre-pandemic individuals displaying a prototypical naïve phenotype compared with the more varied central memory T-cell phenotype observed in COVID-19 patients.<sup>8,9</sup> A24/S<sub>448</sub><sup>+</sup>CD8<sup>+</sup> T cell and A24/S<sub>1208</sub><sup>+</sup>CD8<sup>+</sup> T-cell responses had contrasting TCR $\alpha\beta$  repertoires. While A24/S<sub>448</sub><sup>+</sup>CD8<sup>+</sup> T-cell TCR $\alpha\beta$  repertoire was driven by a common TCR $\beta$  chain motif, the A24/S<sub>1208</sub><sup>+</sup>CD8<sup>+</sup> TCR $\alpha\beta$  repertoire was diverse across COVID-19 patients. As in our recent study,<sup>9</sup> it appears that TCR $\alpha\beta$  diversity might be linked with the prominence of SARS-CoV-2 CD8<sup>+</sup> T-cell responses during the primary infection. The common TCR $\beta$  chain motif recognizing the A24/S<sub>448</sub> and the associated lack of TCR $\alpha\beta$  plasticity are reminiscent of the TCR requirements for the subdominant A2/S<sub>269</sub> epitope<sup>9,24</sup> and in contrast to the diverse TCR $\alpha\beta$  repertoire and promiscuity in TCR $\alpha$ –TCR $\beta$  pairing of the immunodominant HLA-B\*07:02-restricted N<sub>105</sub>-specific CD8<sup>+</sup> T cells.<sup>9</sup>

Overall, our study provides important insights into SARS-CoV-2-specific CD8<sup>+</sup> T-cell responses associated with a highly frequent HLA-A\*24:02 allele and thus contributes to our knowledge on the experimentally verified SARS-CoV-2 CD8<sup>+</sup> T-cell epitopes. Assembling a comprehensive data set on the key CD8<sup>+</sup> T-cell epitopes restricted by the prominent HLA alleles is needed to depict “universal” HLAs in COVID-19 capable of presenting peptides which elicit broadly cross-reactive immunity across a range of emerging variants. Our previous work defined universal HLA class I alleles (A\*02:01, A\*03:01, B\*08:01, B\*18:01, B\*27:05 and



B\*57:01) in influenza, mounting robust CD8<sup>+</sup> T-cell responses against any human influenza A virus circulating over the last century, including the pandemic strains as well as the avian H5N1 and H7N9 viruses.<sup>25</sup> Identification of such universal CD8<sup>+</sup> (and CD4<sup>+</sup>) T-cell epitopes in COVID-19 is needed for the rational design of the next-generation universal COVID-19 vaccines, especially for high-risk groups such as Indigenous people.

## METHODS

### Study participants and ethics statement

This study recruited four convalescent COVID-19 individuals from community infections (mild: CP09, CP34 and CP46; moderate: CP41) and four prepandemic healthy buffy pack donors obtained from the Australian Red Cross LifeBlood (West Melbourne, VIC, Australia). HLA typing was performed (VTIS, Melbourne, VIC, Australia) and all donors were HLA-A\*24:02<sup>+</sup>. Peripheral blood from COVID-19 donors was collected in heparinized tubes and peripheral blood mononuclear cells from peripheral blood and buffy packs were isolated via Ficoll-Paque separation. Experiments conformed to the Declaration of Helsinki Principles and the Australian National Health and Medical Research Council Code of Practice. Written informed consents were obtained from all blood donors prior to the study with ethics approval from The University of Melbourne (#2056689, #2056761, #1955465 and #1443389) and the Australian Red Cross Lifeblood (ID 2015#8) Human Research Ethics Committees.

### Cell lines, peptides and major histocompatibility complex class I tetramers

HLA-A\*24:02-transfected class I-reduced B-lymphoblastoid cells (C1R.A\*24:02 cells) were maintained in RF-10 medium [Roswell Park Memorial Institute-1640 with 10% heat-inactivated fetal calf serum (Gibco, Thermo Fisher Scientific, Carlsbad, CA, USA)] with 0.3 mg mL<sup>-1</sup> hygromycin-B (Life Technologies, Thermo Fisher Scientific).<sup>21,26</sup> SARS-CoV-2 peptides predicted to bind HLA-A\*24:02 using NetCTLpan1.1<sup>27</sup> were purchased from GenScript Biotech (Singapore) and reconstituted in dimethyl sulfoxide (Figure 1a). Tetramers were generated from soluble, biotinylated HLA-A\*24:02 monomers. In brief, HLA  $\alpha$ -heavy chain with a C-terminal BirA biotinylation motif and  $\beta$ 2-microglobulin were expressed and purified as inclusion bodies in *E. coli*, solubilized in 6 M guanidine HCl and refolded with either S<sub>1208</sub> or S<sub>448</sub> peptide, as essentially as described.<sup>8</sup> Purified, fully biotinylated HLA-A24 monomers were stored at -80°C and conjugated to fluorescently labeled streptavidins, phycoerythrin (PE)-streptavidin or allophycocyanin (APC)-streptavidin (BD Biosciences, Franklin Lakes, NJ, USA) at an 8:1 monomer to streptavidin molar ratio to form peptide-major histocompatibility complex class I tetramers.

### Intracellular cytokine staining

Peripheral blood mononuclear cell samples were stimulated with A24/SARS-CoV-2-predicted peptides from two peptide pools (1  $\mu$ M) for 12 days in RF-10 medium (+20 U mL<sup>-1</sup> interleukin-2).<sup>28</sup> Pool 1 contained 12 spike (S) peptides and pool 2 contained 6 membrane (M) and 4 nucleocapsid (N) peptides. On day 12, cells were stimulated with C1R.A\*24:02 cells that were pulsed with individual peptides for 6 h in the presence of GolgiPlug and GolgiStop (BD Biosciences) plus 10 U mL<sup>-1</sup> interleukin-2, and the SARS-CoV-2-reactive CD8<sup>+</sup> T cells were quantified using anti-IFN $\gamma$ -V450 and anti-TNF- $\alpha$ -AF700 in an intracellular cytokine staining assay.<sup>29</sup>

### Ex vivo tetramer-associated magnetic enrichment and TCR analysis

For tetramer-associated magnetic enrichment, cells (5–32  $\times$  10<sup>6</sup>) were incubated with FcR Block (Miltenyi Biotec, Bergisch Gladbach, Germany) and anti-NK1.1 (BD Biosciences)<sup>21</sup> before staining with A24/S<sub>448</sub>-PE and A24/S<sub>1208</sub>-APC tetramers at 1:100 for 1 h in MACS buffer (PBS with 0.5% bovine serum albumin and 2 mM ethylenediaminetetraacetic acid). Tetramer<sup>+</sup> cells were enriched with anti-PE and anti-APC microbeads (Miltenyi Biotec) using magnetic separation.<sup>15,16</sup> Unenriched, enriched and flow-through fractions were stained with anti-CD4-BV650, anti-CD27-BV711, anti-CD14-APC-H7, anti-CD19-APC-H7, anti-CD45RA-FITC, anti-CD8-PerCP-Cy5.5, anti-CD95-PE-CF594 (BD Biosciences), anti-CD3-BV510 (BioLegend, San Diego, CA, USA) and Live/Dead near-infrared (Invitrogen, Carlsbad, CA, USA) for 30 min, washed and resuspended in MACS buffer. Prepandemic samples were acquired on a LSRII Fortessa (BD Biosciences). Enriched tetramer<sup>+</sup> cells from COVID-19 samples were single-cell index-sorted into empty 96-well twin.tec PCR plates (Eppendorf, Hamburg, Germany) using the FACSARIA III (BD Biosciences) for TCR analyses. Plates were kept cold, centrifuged and then stored at -80°C. Amplification of paired CDR3 $\alpha$  and CDR3 $\beta$  regions was performed using multiplex-nested reverse transcription-PCR, as described previously.<sup>15,16</sup> TCR sequences were analyzed using IMGT/V-QUEST and flow cytometry data were analyzed using FlowJo (version 10) software (BD, Ashland, OR, USA). Data visualization was performed in R using packages for circular layout<sup>30</sup> and graphics generation.<sup>31</sup>

## ACKNOWLEDGMENTS

We thank all the participants involved in the study, Robyn Esterbauer, Hannah Kelly, Jane Batten and Helen Kent, for support with the cohort. We thank Anthony Purcell for the C1R.A\*24:02 cell line. This work was supported by the NHMRC Leadership Investigator Grant to KK (#1173871); Research Grants Council of the Hong Kong Special Administrative Region; China (#T11-712/19-N) to KK; the Victorian Government MRFF award (#2002073) to SJK and AKW; MRFF Award (#1202445) to KK; MRFF Award (#2005544) to KK, SJK, JAJ and AKW; NHMRC

program grant #1149990 (SJK) and NHMRC project grant #1162760 (AKW). THON, MK and AKW were supported by NHMRC Emerging Leadership Level 1 Investigator Grants (#1194036 THON; #1195698 MK; #1173433 AKW), SJK was supported by NHMRC Senior Principal Research Fellowship (#1136322). JR is supported by an ARC Laureate fellowship. LH is supported by the Melbourne International Research Scholarship (MIRS) and the Melbourne International Fee Remission Scholarship (MIFRS) from The University of Melbourne. JAJ is supported by an NHMRC Early Career Fellowship (ECF) (#1123673).

## CONFLICT OF INTEREST

The authors declare no competing interests.

## AUTHOR CONTRIBUTION

**Louise C Rowntree:** Conceptualization; Data curation; Formal analysis; Investigation; Methodology; Writing-original draft. **Jan Petersen:** Formal analysis; Methodology; Supervision; Writing-review & editing. **Jennifer A Juno:** Formal analysis; Resources; Writing-review & editing. **Priyanka Chaurasia:** Investigation; Methodology; Writing-review & editing. **Kathleen M Wragg:** Methodology; Writing-review & editing. **Marios Koutsakos:** Formal analysis; Writing-review & editing. **Luca Hensen:** Formal analysis; Methodology; Writing-review & editing. **Adam K Wheatley:** Formal analysis; Writing-review & editing. **Stephen J Kent:** Methodology; Resources; Writing-review & editing. **Jamie Rossjohn:** Methodology; Resources; Supervision. **Katherine Kedzierska:** Conceptualization; Funding acquisition; Resources; Supervision; Writing-original draft. **Thi HO Nguyen:** Conceptualization; Formal analysis; Investigation; Methodology; Supervision; Writing-original draft.

## REFERENCES

- Dong E, Du H, Gardner L. An interactive web-based dashboard to track COVID-19 in real time. *Lancet Infect Dis* 2020; **20**: 533–534.
- Polack FP, Thomas SJ, Kitchin N, *et al.* Safety and efficacy of the BNT162b2 mRNA COVID-19 vaccine. *N Engl J Med* 2020; **383**: 2603–2615.
- Voysey M, Clemens SAC, Madhi SA, *et al.* Safety and efficacy of the ChAdOx1 nCoV-19 vaccine (AZD1222) against SARS-CoV-2: an interim analysis of four randomised controlled trials in Brazil, South Africa, and the UK. *Lancet* 2021; **397**: 99–111.
- Thevarajan I, Nguyen THO, Koutsakos M, *et al.* Breadth of concomitant immune responses prior to patient recovery: a case report of non-severe COVID-19. *Nat Med* 2020; **26**: 453–455.
- Koutsakos M, Rowntree LC, Hensen L, *et al.* Integrated immune dynamics define correlates of COVID-19 severity and antibody responses. *Cell Rep Med* 2021; **2**: 100208.
- Dan JM, Mateus J, Kato Y, *et al.* Immunological memory to SARS-CoV-2 assessed for up to 8 months after infection. *Science* 2021; **371**: eabf4063.
- Wheatley AK, Juno JA, Wang JJ, *et al.* Evolution of immune responses to SARS-CoV-2 in mild-moderate COVID-19. *Nat Comms* 2021; **12**: 1162.
- Habel JR, Nguyen THO, van de Sandt CE, *et al.* Suboptimal SARS-CoV-2-specific CD8<sup>+</sup> T cell response associated with the prominent HLA-A\*02:01 phenotype. *Proc Natl Acad Sci USA* 2020; **117**: 24384–24391.
- Nguyen THO, Rowntree LC, Petersen J, *et al.* CD8<sup>+</sup> T cells specific for an immunodominant SARS-CoV-2 nucleocapsid epitope display high naive precursor frequency and TCR promiscuity. *Immunity* 2021; **54**: 1066–1082.e1065.
- Kared H, Redd AD, Bloch EM, *et al.* SARS-CoV-2-specific CD8<sup>+</sup> T cell responses in convalescent COVID-19 individuals. *J Clin Invest* 2021; **131**: e145476.
- Ferretti AP, Kula T, Wang Y, *et al.* Unbiased screens show CD8<sup>+</sup> T cells of COVID-19 patients recognize shared epitopes in SARS-CoV-2 that largely reside outside the spike protein. *Immunity* 2020; **53**: 1095–1107.e1093.
- Tarke A, Sidney J, Kidd CK, *et al.* Comprehensive analysis of T cell immunodominance and immunoprevalence of SARS-CoV-2 epitopes in COVID-19 cases. *Cell Rep Med* 2021; **2**: 100204.
- Peng Y, Mentzer AJ, Liu G, *et al.* Broad and strong memory CD4<sup>+</sup> and CD8<sup>+</sup> T cells induced by SARS-CoV-2 in UK convalescent individuals following COVID-19. *Nat Immunol* 2020; **21**: 1336–1345.
- Schulien I, Kemming J, Oberhardt V, *et al.* Characterization of pre-existing and induced SARS-CoV-2-specific CD8<sup>+</sup> T cells. *Nat Med* 2021; **27**: 78–85.
- Valkenburg SA, Josephs TM, Clemens EB, *et al.* Molecular basis for universal HLA-A\*0201-restricted CD8<sup>+</sup> T-cell immunity against influenza viruses. *Proc Natl Acad Sci USA* 2016; **201603106**.
- Nguyen TH, Tan AC, Xiang SD, *et al.* Understanding CD8<sup>+</sup> T-cell responses toward the native and alternate HLA-A\*02:01-restricted WT1 epitope. *Clin Transl Immunology* 2017; **6**: e134.
- Ndhlovu ZM, Kanya P, Mewalal N, *et al.* Magnitude and kinetics of CD8<sup>+</sup> T cell activation during hyperacute HIV infection impact viral set point. *Immunity* 2015; **43**: 591–604.
- Messaoudi I, Guevara Patiño JA, Dyal R, LeMaout J, Nikolich-Zugich J. Direct link between MHC polymorphism, T cell avidity, and diversity in immune defense. *Science* 2002; **298**: 1797–1800.
- Price DA, Asher TE, Wilson NA, *et al.* Public clonotype usage identifies protective Gag-specific CD8<sup>+</sup> T cell responses in SIV infection. *J Exp Med* 2009; **206**: 923–936.
- Nguyen TH, Bird NL, Grant EJ, *et al.* Maintenance of the EBV-specific CD8<sup>+</sup> TCR $\alpha\beta$  repertoire in immunosuppressed lung transplant recipients. *Immunol Cell Biol* 2017; **95**: 77–86.
- Hensen L, Illing PT, Bridie Clemens E, *et al.* CD8<sup>+</sup> T cell landscape in Indigenous and non-Indigenous people restricted by influenza mortality-associated HLA-A\*24:02 allomorph. *Nat. Commun.* 2021; **12**: 2931.
- Hertz T, Oshansky CM, Roddam PL, *et al.* HLA targeting efficiency correlates with human T-cell response magnitude and with mortality from influenza A infection. *Proc Natl Acad Sci USA* 2013; **110**: 13492–13497.

23. Nelde A, Bilich T, Heitmann JS, *et al.* SARS-CoV-2-derived peptides define heterologous and COVID-19-induced T cell recognition. *Nat Immunol* 2021; **22**: 74–85.
24. Shomuradova AS, Vagida MS, Sheetikov SA, *et al.* SARS-CoV-2 epitopes are recognized by a public and diverse repertoire of human T cell receptors. *Immunity* 2020; **53**: 1245–1257.e1245.
25. Quinones-Parra S, Grant E, Loh L, *et al.* Preexisting CD8<sup>+</sup> T-cell immunity to the H7N9 influenza A virus varies across ethnicities. *Proc Natl Acad Sci USA* 2014; **111**: 1049–1054.
26. Mei S, Ayala R, Ramarathinam SH, *et al.* Immunopeptidomic Analysis Reveals That Deamidated HLA-bound Peptides Arise Predominantly from Deglycosylated Precursors. *Mol Cell Proteom* 2020; **19**: 1236–1247.
27. Stranzl T, Larsen MV, Lundegaard C, Nielsen M. NetCTLpan: pan-specific MHC class I pathway epitope predictions. *Immunogenetics* 2010; **62**: 357–368.
28. Koutsakos M, Illing PT, Nguyen THO, *et al.* Human CD8<sup>+</sup> T cell cross-reactivity across influenza A B and C viruses. *Nat Immunol* 2019; **20**: 613–625.
29. Clemens EB, Grant EJ, Wang Z, *et al.* Towards identification of immune and genetic correlates of severe influenza disease in Indigenous Australians. *Immunol Cell Biol* 2016; **94**: 367–377.
30. Gu Z, Gu L, Eils R, Schlesner M, Brors B. Circlize implements and enhances circular visualization in R. *Bioinformatics* 2014; **30**: 2811–2812.
31. Wickham H. ggplot2: Elegant Graphics for Data Analysis. New York: Springer-Verlag, 2016.

© 2021 The Authors. *Immunology & Cell Biology* published by John Wiley & Sons Australia, Ltd on behalf of Australian and New Zealand Society for Immunology, Inc

This is an open access article under the terms of the Creative Commons Attribution-NonCommercial-NoDerivs License, which permits use and distribution in any medium, provided the original work is properly cited, the use is non-commercial and no modifications or adaptations are made.